MNRAS **000**, 1–4 (20??) Preprint 12 November 2019 Compiled using MNRAS LATEX style file v3.0

A new method to determine the age of H II regions

TBD,[1]★
[1] *TBD*

Accepted XXX. Received YYY; in original form ZZZ

ABSTRACT

Key words: keyword1 – keyword2 – keyword3

1 INTRODUCTION

McLeod et al. (2019) (M19 thereafter)

- hii regions important - refs?
- ages determination important -refs ?
- loads of different methods to get age: WHAT ARE THEY?
- here trying to work out/test unresolved ages from emission lines with a resolved stellar population, i.e. we can see the stars in 118 and 119 - work out ages and test nebular emission back against what we also detect in the same regions - check ionizing flux output and stellar mass too or something

2 OBSERVATIONS AND MODELS

2.1 Observational Data

?? TALK ABOUT THE INDIVIDUAL HII REGION NAMES ABC ETC... ?? DECIDE LATER WHEN MORE HAS BEEN WRITTEN The stars considered in this work (see Table 1) belong to two giant HII region complexes – D118 and D119 – located within NGC 300 (D~2 Mpc, Z=0.33$Z_\odot$). We remark that the D118 and D119 notation is an abbreviation of the format established by Deharveng et al. (1988) introduced in M19. For consistency with table 3 of M19, however, we conserve the original nomenclature in our Table 1. They were observed by M19 using the Multi Unit Spectroscopic Explorer (MUSE – Bacon et al. 2010) on the Very Large Telescope, and high angular resolution Hubble Space Telescope catalogues were used to de-blend and resolve single stars. Further details on the observations and the data reduction can be found in Section 2 of M19.

In order to derive stellar parameters, M19 fitted the extracted spectra of each star to PoWR atmosphere model grids. As they were solely calculated for Galactic, LMC and SMC metallicities, and given that for NGC 300 $Z \approx 0.33Z_\odot$Butler et al. (2004), the LMC PoWR grids (Z = $0.5Z_\odot$) were the most consistent. The best fit were identified using χ^2 minimisation. One major source of uncertainty is that unresolved binaries are not taken into account – photon fluxes calculated are therefore lower limits. Additionally, the limited number of strong WR star features in the spectra of two of the 4 WR stars observed by M19 led to unconstrained stellar parameters. Therefore they cannot be used in this work.

2.2 BPASS and `hoki`

The Binary Population and Spectral Synthesis –BPASS– models simulate the evolution of stellar populations for a range of metallicities and initial mass functions (IMFs) with the ability to take into account the effects of binary populations. An exhaustive description of the physical prescriptions included in the models can be found in Eldridge et al. (2017); Stanway & Eldridge (2018). In this work we use the outputs of BPASS v2.2.1 with a standard IMF (Salpeter 1955) and a metallicity Z = 0.06 corresponding to ≈ 1/3 $Z_\odot$, which is the closest BPASS metallicity to NGC 300. We also consider Z = 0.08 and Z = 0.10 (i.e. $0.4Z_\odot$and 0.5 $Z_\odot$) since the physical parameters of the stars in M19 were found based on Z = $0.5Z_\odot$PoWR models. We discuss the effects of varying metallicity in Appendix A. **YO METALLICITY MATTER FOR MASS AND STELLAR COUNTS< NEEDS TO HAPPEN IN TEXCT AS WELL- ONLY PUT THE EXTRA PLOTS IN APPENDIX**

The data analysis based on the BPASS outputs was performed using `hoki` v1.2.1-beta[1] (Stevance et al in prep.), a Python package designed to interface with BPASS outputs to facilitate data analysis and comparison to observational data. Jupyter notebooks showing the complete analysis contained within this paper have been made available online for reproducibility purposes[2].

★ E-mail: TBD

[1] https://github.com/HeloiseS/hoki
[2] LALALALA

Table 1. Stellar parameters for the O-type and WR stars considered in this work as obtained by M19 (see their tables 3 and 4) from best-fit PoWR atmosphere models (Hainich et al. 2019). The most likely age of each star according to the probability distribution functions infered from the synthetic HRDs of BPASS are also given – the non-gaussian nature of most of these distributions does not allow us to provide errors bars and we refer the reader to Figure 1.

ID	log(L) ($L_\odot$)	log(T) ($T_\odot$)	Most likely age log(years)			P(6.7 ≤log(age)≤ 6.9)		
			Z=0.06	Z=0.08	Z=0.10	Z=0.06	Z=0.08	Z=0.10
[DCL88]118-1	5.0	4.48	6.9	6.8	6.8	88.1 %	81.3 %	60.9 %
[DCL88]118-2	5.1	4.45	6.7	6.7	6.7	95.7 %	76.2 %	68.7 %
[DCL88]118-3	4.9	4.46	6.8	6.8	6.8	80.3 %	67.4 %	57.6 %
[DCL88]118-4	5.9	4.47	6.5	6.5	6.5	12.7 %	13.5 %	9.5 %
[DCL88]118-WR2	5.3	4.9	6.9	6.8	6.8	87.3 %	73.7 %	97.2 %
[DCL88]119-1	5.0	4.48	6.9	6.8	6.8	88.1 %	81.3 %	60.9 %
[DCL88]119-2	5.4	4.53	6.7	6.7	6.7	98.1 %	76.0 %	58.8 %
[DCL88]119-3	4.3	4.52	6.8	6.7	6.7	57.3 %	47.3 %	36.3 %
[DCL88]119-3b	5.7	4.52	6.7	6.5	6.5	70.4 %	28.9 %	17.2 %
[DCL88]119-4	4.5	4.52	6.9	6.9	6.9	61.2 %	58.1 %	54.8 %
[DCL88]119-5	4.5	4.56	7.3	7.3	7.3	3.7 %	3.1 %	3.8 %
[DCL88]119-6	4.9	4.46	6.8	6.8	6.8	80.3 %	67.4 %	57.6 %
[DCL88]119-7	4.5	4.52	6.9	6.9	6.9	61.2 %	58.1 %	54.8 %
[DCL88]119-8	4.3	4.52	6.8	6.7	6.7	57.3 %	47.3 %	36.3 %
[DCL88]119-9	4.5	4.52	6.9	6.9	6.9	61.2 %	58.1 %	54.8 %
[DCL88]119-WR1	5.3	4.65	6.9	6.9	6.9	84.5 %	81.3 %	76.3 %

3 RESULTS

3.1 Stellar age estimate from HRDs

One of the outputs of the BPASS models is an ensemble of Hertzsprung-Russell Diagrams (HRD) for each combination of IMF and Z covering 51 time bins ranging from 10^6 to 10^{11} years[3]. Each pixel of a BPASS HRD grid contains a value representing the probability of a star being found in that particular location at a give age, IMF and metallicity.

Using the luminosities and temperatures inferred by M19 – see Table 1 – we can identify which grid element corresponds to each star. By considering all time steps, we can then build a probability distribution function (PDF) indicating the most likely age of a star found at a given location on the HRD.

Doing this for all stars listed in Table 1, we obtain the PDFs shown in Figure 1. The most likely age peak of the distribution) for each star is also summarised Table 1. The non-Gaussian nature of most of these PDFs means that the standard deviation cannot be used as an error bar.

As we can see in Figure 1 and Table 1, most stars have similar ages between 5 and 8 Myrs (log(age)=6.7-6.9). Only 118-4 and 119-5 deviate from this trend, being respectively younger (3 Myrs) and older (20 Myrs) than the rest of the population. Additionally, we can see that the PDF corresponding to the location of 119-WR2 on the HRDs exhibits a small peak at 100 Myrs; an unphysical age for a Wolf-Rayet star. We will first discuss these outliers before attempting to combine the individual PDFs to infer the most likely age of D118 and D119.

[3] Note that the bins are uniformly distributed in log(age) space

3.2 Outliers

3.2.1 118-4

As seen in the Figure 1, the position of 118-4 on the HR diagram correspond to a most likely age that is younger (log(age)=6.7 years, equivalent to ~3 Myr) than all other stars in D118 and D119, which typically prefer ages around 5–8 Myrs. The asymmetric probability distribution functions of some stars in our sample do extend down to very early ages that overlap with 118-4 – that is the case for 119-3,4,7,8 and 9. However, if we calculate the probability that a star has a log(age) between 6.7 and 6.9 years, we can see that all of these other targets have ~a 60-70 per cent chance of being in that age range, whereas 118-4 only has a 3.7 per cent probability. Consequently, it is highly likely that 118-4 genuinely is, or *appears*, younger.

If we consult MC19, particularly their Figure 5, we can see that 118-4 is located away from most stars in D118, which could indicate that it formed at a slightly later date. However, 118-2 and 118-WR2 are also somewhat isolated, and their most likely ages are consistent with the other stars in this region.

Another way to explain the youthful appearance of 118-4 is through rejuvination: if the star underwent a merger event, or accreted a substantial amount of material from a binary companion, it would present as a younger star **(REF)**. The fact that MC19 find this source to be the most massive in their sample count hint that it is the result of a stellar merger.

3.2.2 119-5

Contrary to 118-4, 119-5 appears much older than the other sources in our sample, with most likely log(age)=7.3 years (~20 Myrs) which is too old for a source in an H II region. In Figure 9 of MC19 we can see that 119-5 is located away from the core of 119-A inhabited by 119-3,4,6,8 and

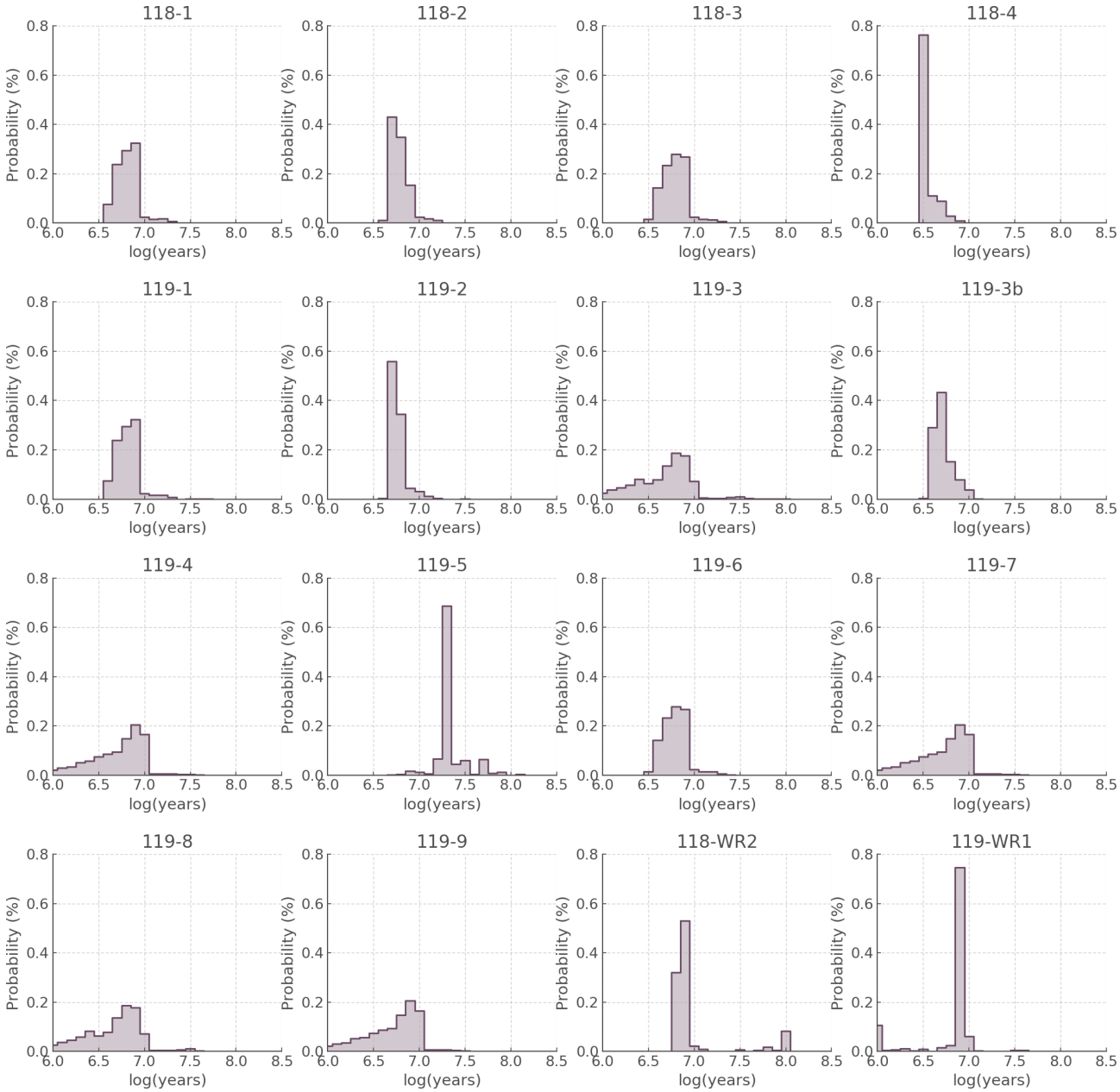

Figure 1. Probability distribution functions of the age of each star inferred from the stellar parameters quoted in Table 1 and the synthetic HRDs of BPASS for a standard IMF and a metallicity $Z = 0.06$. The most likely age of each star is summarised in Table 1.

9. Either background or foreground star, or something is lowering temperature and luminosity => DUST? **COULD THIS BE BACKGROUND OR FOREGROUND? ASK ANNA AGAIN**

3.2.3 119-WR2

Althought the probability distribution function of 119-WR2 indicates a most likely age (log(age)=6.9) that is consistent with that of the other stars in the sample, and an 84.5 per cent probability of having a log(age) between 6.7 and 6.9 yrs (~5–8 Myrs), a peculiar speak can be seen in the PDF at log(age) = 8.0. This corresponds to an age of ~100 Myrs, which is not physical for WR stars and inconsistent with the age of the rest of the population.

This age spike can be explained by the presence of helium star in the BPASS models which are found in the same region of the HRDs but at later times.

3.3 Aggregate age

In order to estimate the age of D118 and D119 we multiply the PDFs of the stars in these regions, omitting 118-4 and 119-5 since they have been identified as outliers (see Section 3.2).

In Figure 2 we present the PDFs of the ages of D118 and D119 based on our sample including and excluding the WR

stars. The position of the WR stars on the HRD gives them quite narrow PDFs which can drastically change the shape of the aggregate PDFs. In the case of D118 the inclusion of WR stars even brings the probability of the log(age)=6.7 bin to zero. In D119, no age bin is excluded when including the WR stars, but one log(age) comes to dominate significantly (6.9). Overall, the inclusion of the WR stars narrows the aggregate PDFs for the ages of our HII regions.

Given the uncertainties on the temperature estimates of WR stars, we are reluctant to conclude that the log(age)=6.7 bin should be excluded for D118, or that log(age)=6.9 should become dominant with over 80 per cent confidence solely based on the inclusion of one WR star in each of these regions. The combined age of D118 and D119 is also sensitive to whether we include the WR stars in our sample or not. Excluding the WR stars, the most likely age is found to be log(age)=6.8 with 80 per cent confidence, whereas if they are taken into account, we find log(age)=6.9 with >95 per cent confidence. We caution that these confidence intervals are solely based on the BPASS models and do not reflect the uncertainties that will inevitably propagate from the estimation of the stellar parameters.

4 ANALYSIS OR DISCUSSION???

4.1 Stellar numbers: observations Vs theory

Overall, MC19 found 13 O stars and 4 WR stars (two of which are not considered in the present study – see Section **??**). By comparing these figure to the number of O and WR stars in BPASS we can provide an estimate of the stellar mass and stellar counts, given the standard IMF (see Section 2.2). (**DO ALL METALLICITIES IN A TABLE)**)

- O and WR numbers and the ratio and how the sample is probably incomplete and so the stellar mass and numbers are LOWER ESTIMATES.

4.2 Ionizing flux

4.3 Predicted age and BPT diagrams

- something something, calcualtion of the line ratios - plots

5 DISCUSSION AND CONCLUSIONS

ACKNOWLEDGEMENTS

The Acknowledgements section is not numbered. Here you can thank helpful colleagues, acknowledge funding agencies, telescopes and facilities used etc. Try to keep it short.

REFERENCES

Bacon R., et al., 2010, in Proc. SPIE. p. 773508, doi:10.1117/12.856027
Butler D. J., Martínez-Delgado D., Brandner W., 2004, AJ, 127, 1472
Deharveng L., Caplan J., Lequeux J., Azzopardi M., Breysacher J., Tarenghi M., Westerlund B., 1988, A&AS, 73, 407
Eldridge J. J., Stanway E. R., Xiao L., McClelland L. A. S., Taylor G., Ng M., Greis S. M. L., Bray J. C., 2017, Publ. Astron. Soc. Australia, 34, e058
Hainich R., Ramachandran V., Shenar T., Sand er A. A. C., Todt H., Gruner D., Oskinova L. M., Hamann W. R., 2019, A&A, 621, A85
McLeod A. F., et al., 2019, arXiv e-prints, p. arXiv:1910.11270
Salpeter E. E., 1955, ApJ, 121, 161
Stanway E. R., Eldridge J. J., 2018, MNRAS, 479, 75

APPENDIX A: THE EFFECTS OF METALLICITY

Put figures here and say the age determination would barely change :)

This paper has been typeset from a TEX/LATEX file prepared by the author.

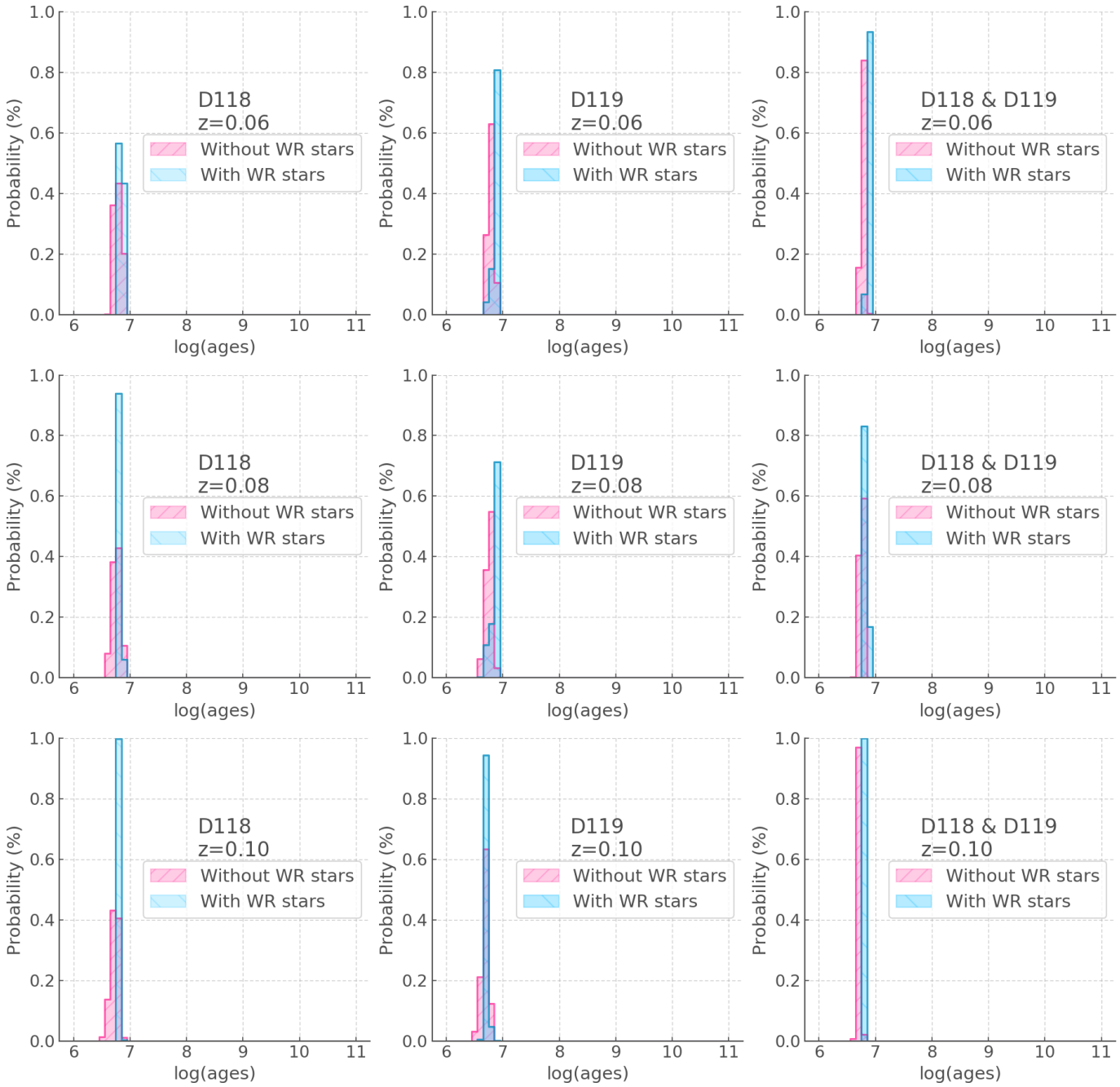

Figure 2. Probability distribution functions of D118 and D119 produced from the combination of the PDFs in Figure 1, not including 118-4, 119-5.

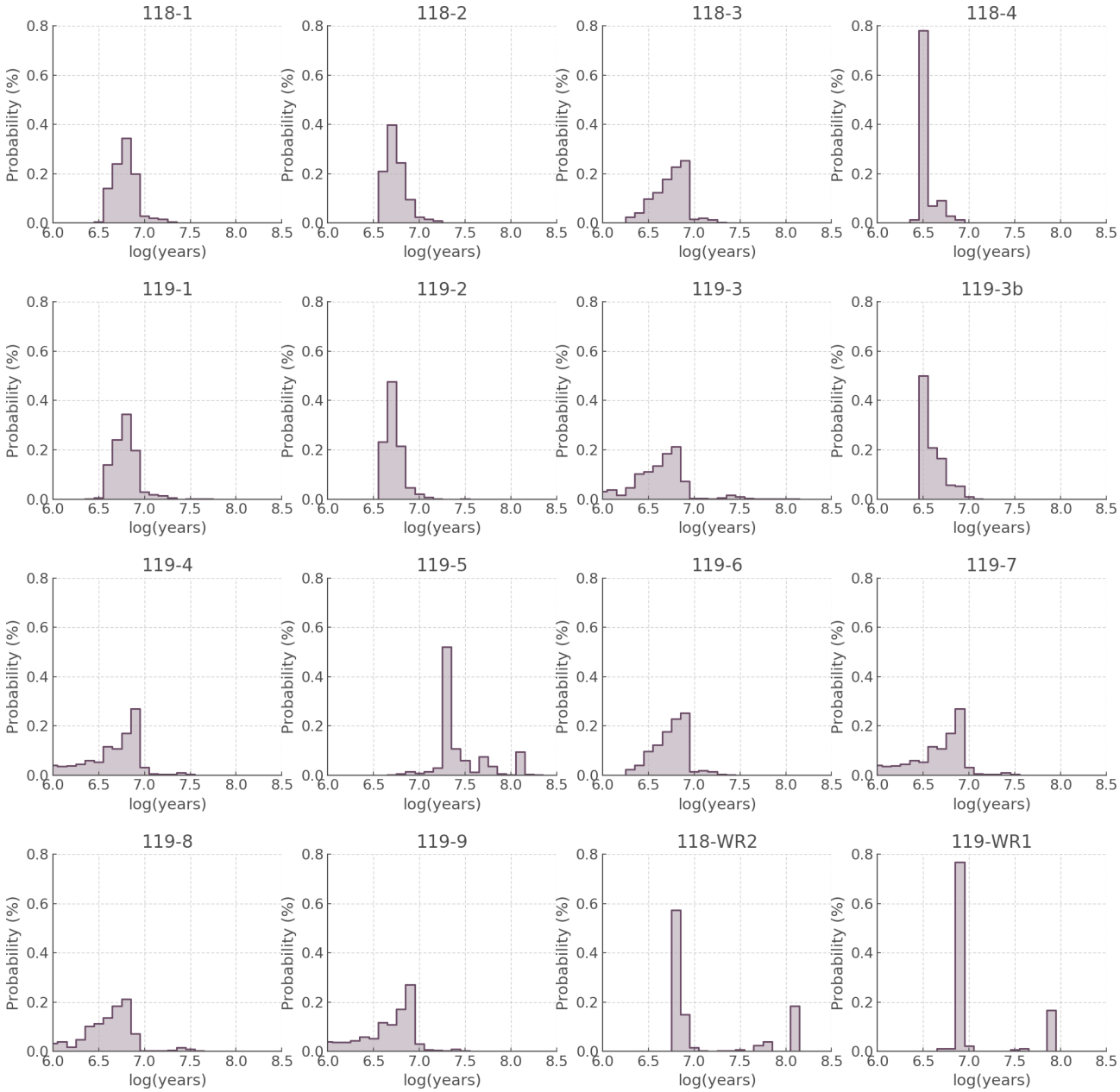

Figure A1. Probability distribution functions of the age of each star inferred from the stellar parameters quoted in Table 1 and the synthetic HRDs of BPASS for a standard IMF and a metallicity $Z = 0.08$. The most likely age of each star is summarised in Table 1.

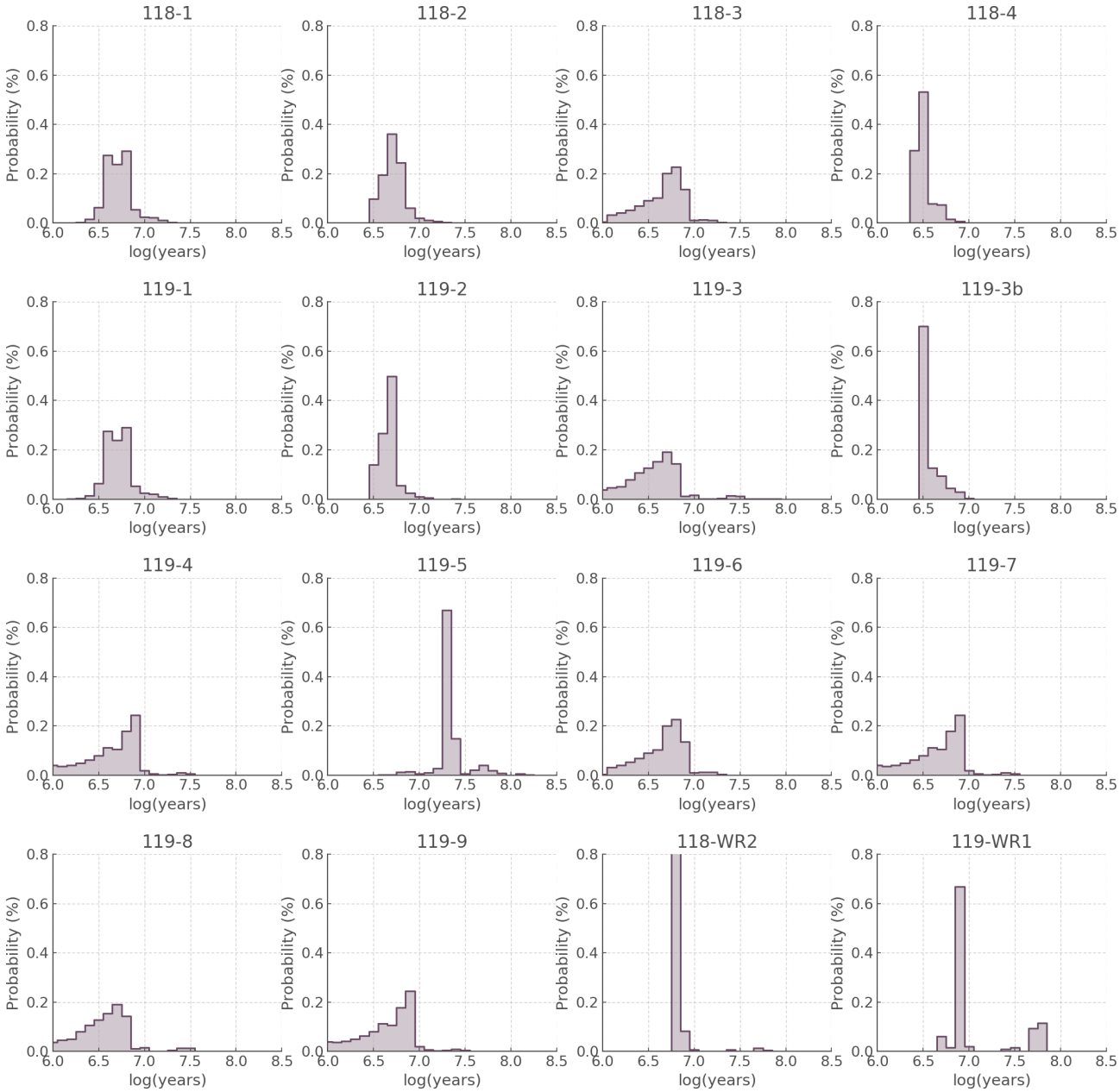

Figure A2. Probability distribution functions of the age of each star inferred from the stellar parameters quoted in Table 1 and the synthetic HRDs of BPASS for a standard IMF and a metallicity $Z = 0.10$. The most likely age of each star is summarised in Table 1.